The EMBO Journal (2008) 27, 2411–2421 | © 2008 European Molecular Biology Organization | Some Rights Reserved 0261-4189/08
www.embojournal.org

THE EMBO JOURNAL

EMBO open

Mutations of RNA polymerase II activate key genes of the nucleoside triphosphate biosynthetic pathways

Marta Kwapisz[1,2,4], Maxime Wery[1,4], Daphné Després[1], Yad Ghavi-Helm[1], Julie Soutourina[1], Pierre Thuriaux[1,*] and François Lacroute[2,3]

[1]CEA, iBiTec-S, Service de Biologie Intégrative et Génétique Moléculaire, Gif-sur-Yvette, France, [2]CNRS, Centre de Génétique Moléculaire, UPR2167, Gif-sur-Yvette, France and [3]Université Pierre et Marie Curie, Paris, France

The yeast *URA2* gene, encoding the rate-limiting enzyme of UTP biosynthesis, is transcriptionally activated by UTP shortage. In contrast to other genes of the UTP pathway, this activation is not governed by the Ppr1 activator. Moreover, it is not due to an increased recruitment of RNA polymerase II at the *URA2* promoter, but to its much more effective progression beyond the *URA2* mRNA start site(s). Regulatory mutants constitutively expressing *URA2* resulted from *cis*-acting deletions upstream of the transcription initiator region, or from amino-acid replacements altering the RNA polymerase II Switch 1 loop domain, such as *rpb1-L1397S*. These two mutation classes allowed RNA polymerase to progress downstream of the *URA2* mRNA start site(s). *rpb1-L1397S* had similar effects on *IMD2* (IMP dehydrogenase) and *URA8* (CTP synthase), and thus specifically activated the rate-limiting steps of UTP, GTP and CTP biosynthesis. These data suggest that the Switch 1 loop of RNA polymerase II, located at the downstream end of the transcription bubble, may operate as a specific sensor of the nucleoside triphosphates available for transcription.

The EMBO Journal (2008) **27,** 2411–2421. doi:10.1038/emboj.2008.165; Published online 21 August 2008
Subject Categories: chromatin & transcription
Keywords: IMD2; IMD3; *S. cerevisiae*; URA2; URA8

Introduction

DNA transcription depends on the availability of pyrimidine (UTP and CTP) and purine (GTP and ATP) ribonucleoside triphosphate substrates, and their *de novo* synthesis is subjected to tight homoeostatic controls. In yeast, the first two steps of UTP biosynthesis are catalysed by Ura2, a bifunctional protein endowed with carbamoyl phosphate synthetase and aspartate transcarbamoylase activities (Potier *et al*, 1987). These are the main rate-limiting steps of the pathway, and their allosteric control by UTP is well documented (Lacroute *et al*, 1965; Serre *et al*, 2004). Similar to other genes of the UTP biosynthetic pathway, *URA2* transcription is induced in the presence of 6-azauracil, which depletes cells in UTP (Exinger and Lacroute, 1992). A previous study (Losson and Lacroute, 1981) has suggested that this does not depend on Ppr1, a transcriptional activator specific for the pyrimidine biosynthetic pathway (Loison *et al*, 1980; Losson and Lacroute, 1981; Flynn and Reece, 1999), as *ppr1-2*, a mutation unable to activate *URA1* or *URA3*, had no effect on Ura2 activity in cell-free extracts. Moreover, we here show that a *ppr1*Δ null allele remains fully competent for *URA2* transcription.

In this study, two classes of mutations were found to constitutively activate *pURA2*::*HIS3* or *pURA2*::*LacZ* reporter plasmids. The first class was due to short deletions immediately upstream of the *URA2* mRNA 5′-ends, indicating that this region acts as negative regulatory element of *URA2* transcription. A second class altered *RPB1*, which encodes the largest subunit of RNA polymerase II, and specifically modified the Switch 1 loop of the active site. One of these mutations, *rpb1-L1397S*, was investigated in more detail. It showed a genome-wide reduced occupancy of RNA polymerase II, consistent with its partial growth defect, but specifically activated *URA2, IMD2/IMD3* and *URA8* (encoding rate-limiting steps of the UTP, GTP and CTP biosynthetic pathways, respectively), thus raising the intriguing possibility that the Switch 1 loop of RNA polymerase II might act as a sensor of nucleoside triphosphate depletion.

Results

UTP depletion activates URA2 independently of the Ppr1 activator

The *URA2* open reading frame is separated by 1231 nt from the stop codon of the upstream gene *TRK1* (Figure 1A). A *Kpn*I–*Bam*HI cassette bearing this DNA was cloned in frame with the *LacZ* or *HIS3* open reading frames, generating the *pURA2*::*LacZ* reporter plasmids pFL80 and pFL80-H2, and the *pURA2*::*HIS3* reporter pFL81 (Materials and methods). There was a fivefold *LacZ* activation in wild-type cells grown under repressing (uracil) or derepressing (6-azauracil) conditions (Figure 1B), and a similar range of activation was observed in the steady-state level of *URA2* mRNAs (Figure 1C), indicating that the *pURA2*::*LacZ* reporter correctly reflects the transcriptional regulation of *URA2*.

*Corresponding author. CEA, iBiTec-S, Service de Biologie Intégrative et Génétique Moléculaire, Gif sur Yvette F-91191, France.
Tel.: +33 1 69 08 35 86; Fax: +33 1 69 08 47 12;
E-mail: pierre.thuriaux@cea.fr
[4]These authors contributed equally to this work

Received: 2 June 2008; accepted: 30 July 2008; published online: 21 August 2008

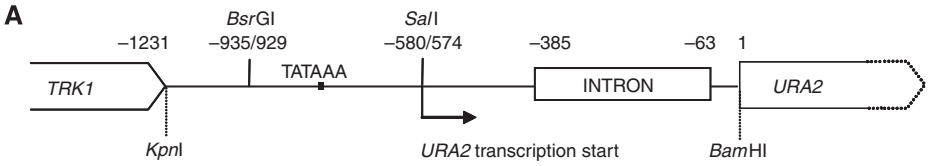

B

Strain	Growth conditions	β-Galactosidase
BMA64-URA3 (WT)	CSM+U	2.9
	CSM	9.4
	CSM+MPA (50 mg/L)	6.9
	CSM+6AU (20 mg/L)	13.6
BMA64-URA3 (WT)	CSM 34 °C	10.7
FL55 (*ura8-ts ura7*Δ)	CSM 34 °C	1.8

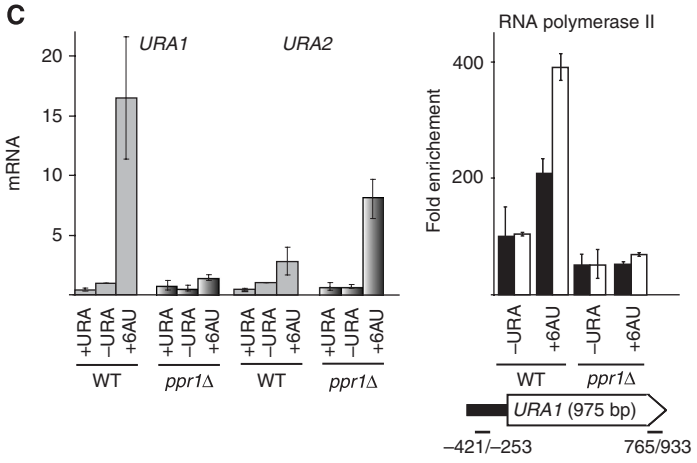

Figure 1 Transcriptional regulation of *URA2* in response to UTP shortage. (**A**) Schematic view of the *TRK1–URA2* intergenic region. The corresponding DNA was cloned as a *Kpn*I–*Bam*HI cassette to generate the pFL80 and pFL80-H2 *pURA2*::*LacZ* reporter plasmids. A box denotes the 5′-UTR intron. The broken arrow corresponds to the *URA2* mRNAs 5′-ends. (**B**) β-galactosidase activities of BMA64-URA3 (WT) and FL55 (*ura8-ts ura7*Δ) grown without uracil (CSM) at 30 and 34 °C, in the presence of uracil (CSM + U), mycophenolate (CSM + MPA) and 6-azauracil (CSM + 6AU). (**C**) Three independent cultures of BMA64-URA3 (WT) and FL53 (*ppr1*Δ) were exponentially grown without (−URA) or with uracil (+URA), or with 200 mg/l of 6-azauracil (+6AU). *URA1* and *URA2* mRNAs were quantified by RT–PCR, and RNA polymerase II occupancy was determined by ChIP assays, using anti-CTD antibodies (8WG16). A schematic map represents the *URA1* gene, with the oligonucleotide pairs used as primers. Position 1 corresponds to the start codon.

Adding 6-azauracil blocks UTP synthesis and also reduces the cellular pool of GTP (Exinger and Lacroute, 1992). However, no *pURA2*::*LacZ* activation was observed in the presence of mycophenolate, which specifically blocks IMP dehydrogenase (Shaw *et al*, 2001), and thus only depletes GTP. Likewise, counteracting GTP inhibition by adding guanine to the CSM + 6AU medium did not reduce the activating effect of 6-azauracil (data not shown). Finally, impairing the metabolic conversion of UTP to CTP in temperature-sensitive mutant (*ura8-ts ura7*Δ) reduced the expression of *pURA2*::*LacZ*, which presumably reflects the accumulation of UTP under these conditions and implies that *URA2* does not respond to CTP shortage. These data indicated that *URA2* transcription is primarily activated by a shortage in UTP, with little or no effect of GTP or CTP.

Other genes of the pyrimidine pathway, such as *URA1* and *URA3*, are also derepressed under UTP depletion, and their activation is lost in *ppr1-2*, a mutation that alters the Ppr1 activator but has no effect on the Ura2 activity in cell-free extracts (Losson and Lacroute, 1981). Consistent with this observation, we found here that the *ppr1*Δ null allele strongly reduced the activation of *URA1* and *URA3* in the presence of 6-azauracil, as measured by RT–PCR quantification of their mRNAs and by their RNA polymerase II occupancy in chromatin-immunoprecipitation (ChIP) assays (shown in Figure 1C for the *URA1* gene). In contrast, *ppr1*Δ actually increased the level of *URA2* mRNA produced in the presence of 6-azauracil, which may reflect a particularly effective depletion in UTP, due to its inability to activate *URA1* and *URA3*.

Organisation of the URA2 promoter region

It was previously thought that *URA2* transcription starts some 70 nt ahead of the ATG start codon (Potier *et al*, 1990). This is clearly inconsistent with the recent report of an untranslated intron between positions −385 and −66 relatively to the ATG (Juneau *et al*, 2007). As shown in Figure 2, we confirmed the existence of this intron, although with different 3′-ends corresponding to positions −63, −54 or, in one case, +12. The corresponding DNA has a 5′-end consensus ($_{-384}$GUAUGU$_{-379}$), a canonical branch point box ($_{-92}$UACUAAC$_{-84}$), and a $_{-68}$UAG$_{-65}$ at the 3′-splice site. An intron deletion did not detectably affect the expression of *pURA2*::*LacZ* (bottom line of Figure 2A).

Using RNA ligase mediated-RACE assays, we obtained and sequenced 13 cDNAs that, by construction, extended to position +188 of the *URA2* open reading frame and thus corresponded to the 5′-end domains of full-length mRNAs (Figure 2B). These 5′-ends defined six positions (−588A, −579T, −576A, −571A, −565A and −563A) clustered within an A-rich domain, matching to the initiator consensus $(A_{rich})_5N(C/T)\underline{A}(A/T)NN(A_{rich})_6$ deduced from a recent survey of yeast mRNAs (Zhang and Dietrich, 2005). A parallel study (Thiebaut *et al*, 2008) has identified a second initiator region (positions −686/−657, denoted by a grey arrow in Figure 2A) upstream of the one shown here to be used for full-length *URA2* mRNAs. This upstream initiator produces short unstable non-coding RNAs with the same transcriptional orientation as *URA2*. It is evidently not used to produce full-length *URA2* transcripts, as the predicted 5′-ends were not found in the corresponding cDNAs (Figure 2B). Five TCTT (UCUU) boxes, present immediately upstream of the

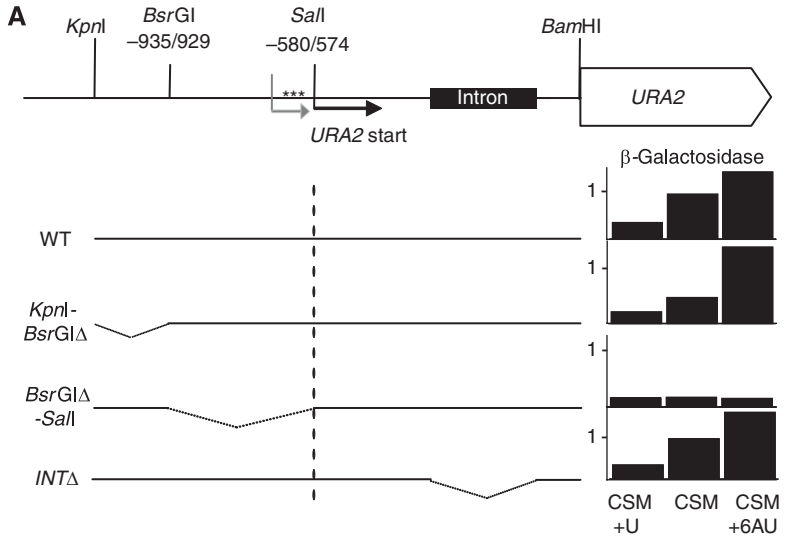

B

–589AAAAAACCTgtcgacAACAACCACAAAC–563

Start	Intron		cDNA
–588	–384	–63	wt (CSM+U)
–579	–384	–54	
–576	–384	–54	
–588	–384	–54	wt (CSM+6AU)
–588	–384	–54	
–579	–384	–54	
–576	–384	–54	
–571	–384	+12	
–565	–384	–54	
–579	–384	–63	*rpb1-L1397S* (CSM)
–579	–384	–54	
–565	–384	–63	
–563	–384	–63	

Figure 2 Organisation of the *URA2* promoter region. (**A**) Deletion mutagenesis of promoter region. *LacZ* expression in BMA64-URA3 (WT) transformed with pFL80 (*pURA2*::*LacZ*), pFL80-KBΔ (*Kpn*I–*Bsr*GI deletion), pFL80-BSΔ (*Bsr*GI–*Sal*I deletion) and pFL80-INTΔ (no intron). Strains were exponentially grown without (−URA) or with uracil (+URA), or with 200 mg/l of 6-azauracil (+6AU). β-galactosidase was expressed in arbitrary units (Miller, 1972), where 1.0 is the level measured in wild-type cells grown in CSM. Broken arrows correspond to the transcriptional initiator regions, shown in black for full-length *URA2* mRNA and in grey for short upstream untranslated RNAs (Thiebaut *et al*, 2008). A canonical TATAAA box and a cluster of TCTT (UCUU) motifs (stars) are also indicated (see Supplementary data). (**B**) Identification of the *URA2* 5′-end region and of an *URA2* intron. Thirteen cDNAs primed from an oligonucleotide corresponding to positions 167/188 of the *URA2* open reading frame were amplified by the RNA Ligase Mediated-RACE technique (Materials and methods). The six *URA2* start sites (underlined) fall between positions −589 and −563, containing the unique *Sal*I site (*gtcgac*). Nine cDNAs were extracted and amplified from wild-type cells (BMA64-URA3) grown without uracil (−URA), or with 200 mg/l of 6-azauracil (+6AU), and four others were prepared from FL-M9 (*rpb1-L1397S*) grown without uracil (−URA). This also confirmed the existence of an intron between positions −385 and −66 (Juneau *et al*, 2007), but with 3′-borders corresponding to positions −63, −54 or, in one case, +12.

URA2 initiator, form a cluster of binding sites recognised by Nab3, which belongs to the transcriptional terminator system operating on non-coding intergenic RNAs (Arigo *et al*, 2006; Thiebaut *et al*, 2006).

The DNA upstream of the URA2 initiator prevents the progression of RNA polymerase II

Partial deletions of the *TRK1-URA2* intergenic region were introduced in *pURA2*::*LacZ* reporters (pFL80 and pFL80-H2) and tested for *LacZ* activation under repressing (uracil) and derepressing (6-azauracil) conditions. Deleting the first 297 nt had no effect on *pURA2*::*LacZ*, but a *Bsr*GI/*Sal*I deletion lacking positions −934/−580 almost entirely blocked *pURA2*::*LacZ* expression (Figure 2A). The corresponding DNA is therefore critical for *URA2* transcription. It contains a TATAAA box (−776/−771) shown by Thiebaut *et al* (2008) to be needed for the synthesis of the *URA2* mRNA and of its short-lived upstream transcripts.

The *Bsr*GI/*Sal*I DNA was submitted to error-prone amplification and recombined into the *pURA2*::*HIS3* reporter (pFL83), producing plasmids that were selected for *HIS3* overexpression in the presence of uracil. No single-base mutation was isolated by this approach, but we obtained three very similar deletions *up2*Δ (−647/−577), *up6*Δ (−634/−579) or *up10*Δ (−650/−579) upstream of the *Sal*I site (Figure 3A). These deletions overexpressed *LacZ* when subcloned into *pURA2*::*LacZ* reporters (pFL80-H2 and pFL80), and a chromosomal *up2*Δ mutant (FL51) constitutively expressed the *URA2* mRNA under-repressing conditions (Figure 3B). Moreover, *up2*Δ only acted in *cis*, as the

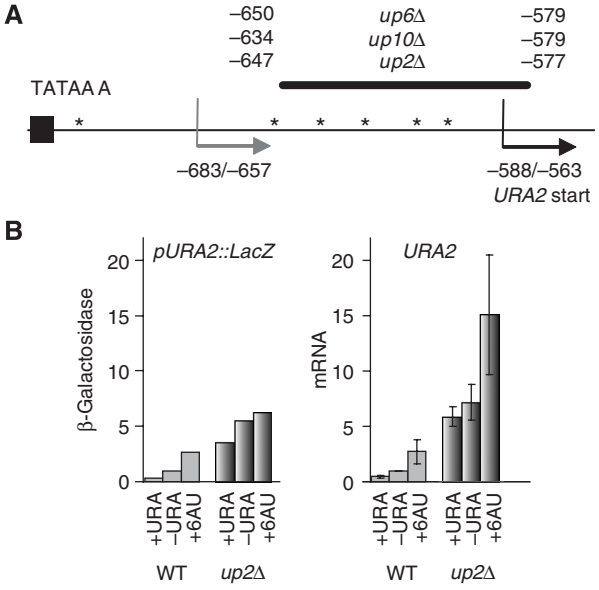

Figure 3 The DNA upstream of the transcription start impairs *URA2* expression. (**A**) Schematic organisation of the *up*Δ mutations. Thick black line corresponds to the deleted DNA *up2*Δ, *up6*Δ and *up10*Δ. Stars indicate TCTT (UCUU) boxes. Broken arrows correspond to the transcriptional initiator regions as shown in Figure 2A. (**B**) Effect of *up2*Δ on *pURA2*::*LacZ* expression and *URA2* mRNA steady-state level. BMA64-URA3 (WT) was transformed with pFL80 or pFL80-up2Δ. β-galactosidase was tested as shown in Figure 2A. *URA2* mRNA is expressed in arbitrary units (Miller, 1972), where 1.0 corresponds to wild-type cells grown in the absence of uracil (−URA). RT–PCR assays are based on three independent cultures of BMA64-URA3 (WT) and FL51 (*up2*Δ), grown with (+URA) or without uracil (−URA), or containing 200 mg/l of 6-azauracil (+6AU).

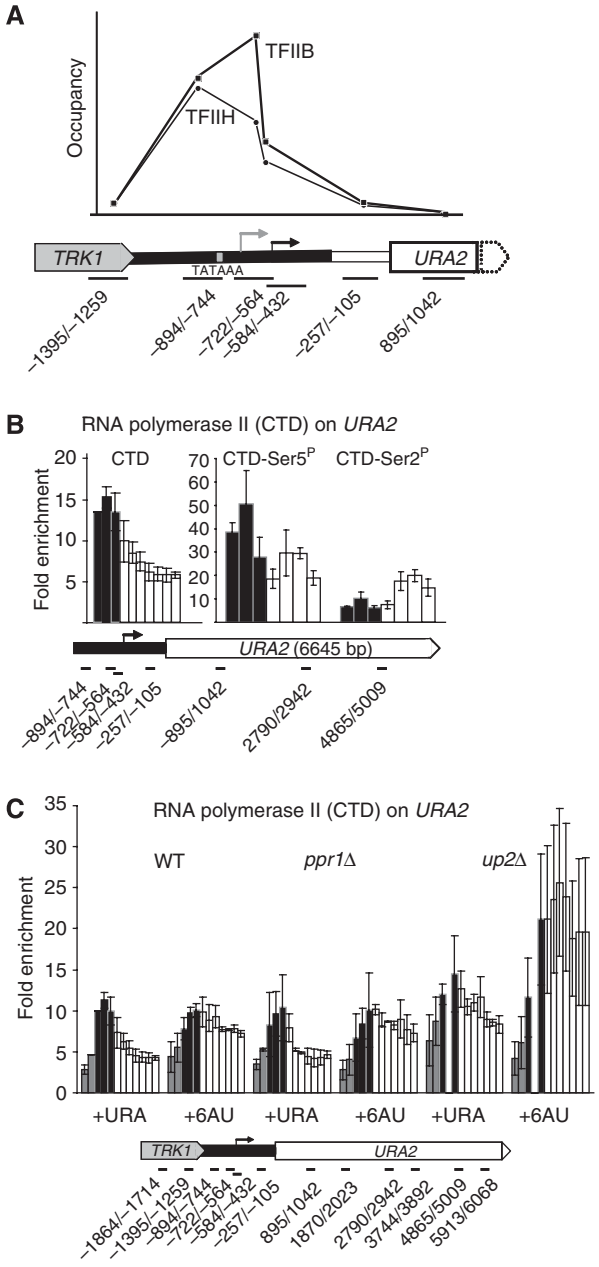

Figure 4 Distribution of TFIIB, TFIIH and RNA polymerase II at the *URA2* locus. (**A**) TFIIH (Rad3-TAP) and TFIIB (Sua7-TAP) were detected by ChIP assays as described in Materials and methods. Strains D712-10C (WT *RAD3*::*TAP*) and D714-5D (WT *SUA7*::*TAP*) were grown on SD + aa. The schematic organisation of the corresponding DNA is presented below. Broken arrows represent the *URA2* mRNA start sites and the upstream initiator, as in Figure 2A. (**B**) RNA polymerase II was immunoprecipitated with Dynabeads anti-mouse (Dynal Biotech), using anti-CTD (8WG16), anti-Ser2^P and anti-Ser5^P antibodies (Covance). Strain GR44-11C (WT) was grown on SD + aa. A schematic map indicates the oligonucleotides used as primers. (**C**) RNA polymerase II occupancy in wild-type, *ppr1*Δ and *up2*Δ. Strains GR44-11C (WT), FL53 (*ppr1*Δ) and FL51 (*up2*Δ) were grown at 30 °C on SD + aa with 2 g/l of uracil (+URA) or exposed to 200 mg/l of 6-azauracil (+6AU). ChIP signals were detected with anti-CTD antibodies (8WG16). A schematic map represents the *URA2* gene, with the oligonucleotides used as primers.

promoter reporter (*pURA2*::*LacZ*) was not activated in the *up2*Δ host (data not shown).

The ChIP assays of Figure 4A show that the region upstream of the *URA2* start site is occupied by TFIIB and TFIIH, two components of the RNA polymerase II pre-initiation complex. The corresponding RNA polymerase II signal was recognised by anti-CTD antibodies, and also by an anti-Rpb3::HA tag (see Figure 7D below), but not by antibodies raised against Ser2-phosphorylated CTD (Figure 4B). The CTD-Ser2^P signal was only detected downstream of the *URA2* initiator region. As shown in Figure 4C, this also coincided with a drop in RNA polymerase II occupancy, observed in wild-type or *ppr1*Δ cells grown under repressing conditions.

URA2 activation in wild-type or *ppr1*Δ cells exposed to 6-azauracil did not increase the RNA polymerase II signal detected upstream of the initiator region, but correlated with a full occupancy of the *URA2* open reading frame by RNA polymerase II (Figure 4C). Likewise, the *up2*Δ mutation produced a strong RNA polymerase II signal downstream of the initiator, even when grown under repressive conditions (Figure 4C). Thus, *URA2* activation is not due to an increased recruitment of RNA polymerase II (as in the case of Ppr1-dependent genes such as *URA1*; see Figure 1C) but results from an extended RNA polymerase II occupancy downstream of the *URA2* initiator region. Moreover, a relatively short DNA region, lost in *up2*Δ and located immediately upstream of the *URA2* initiator, impairs *URA2* transcription by preventing RNA polymerase II from progressing towards the *URA2* open reading frame.

Mutants of the RNA polymerase II Switch 1 loop activate URA2 expression

To search for *trans*-acting regulator(s) of *URA2*, mutations constitutively expressing the chromosomal *pURA2*::*HIS3* reporter of strain FL52 were selected after UV mutagenesis. We obtained four mutants (FL-M9, M10, M13 and M23) that were resistant to 3-aminotriazol on uracil-supplemented medium and also overexpressed the *pURA2*::*LacZ* reporter. They grew slowly at 30 °C, failed to grow at 16 °C and 37 °C and were somewhat sensitive to 6-azauracil (shown in Figure 5A for the FL-M9 strain). Meiotic tetrad analysis showed that these phenotypes co-segregated in a monogenic and recessive way, and complementation tests established that the corresponding mutations belonged to one and the same gene.

We then transformed FL-M9 with a yeast genomic library and obtained one plasmid restoring growth at 37 °C. The corresponding insert harboured *RPB1*, which encodes the largest subunit of RNA polymerase II, and three surrounding genes. Further subcloning showed that growth at 37 °C correlated with an intact *RPB1* gene, and complementation tests with the temperature-sensitive allele *rpb1-1* (Scafe *et al*, 1990) firmly established that all four mutants were due to *rpb1* mutations. *In vivo* gap repair (Rothstein, 1991) indicated that these mutations belonged to the *Swa*I–*Psh*AI segment of *RPB1*. Finally, DNA sequencing revealed single amino-acid replacements corresponding to *rpb1-L1397S* (M9), *rpb1-S1401P* (M10) and *rpb1-F1402L* (M13 and M23), which were also present in the chromosomal DNA of the original mutant strains.

The above-mentioned data led to the rather unexpected conclusion that *URA2* activation occurs by *trans*-acting mutations altering RNA polymerase II itself, at the level of its Switch 1 loop fold. RT–PCR and *LacZ* assays confirmed that

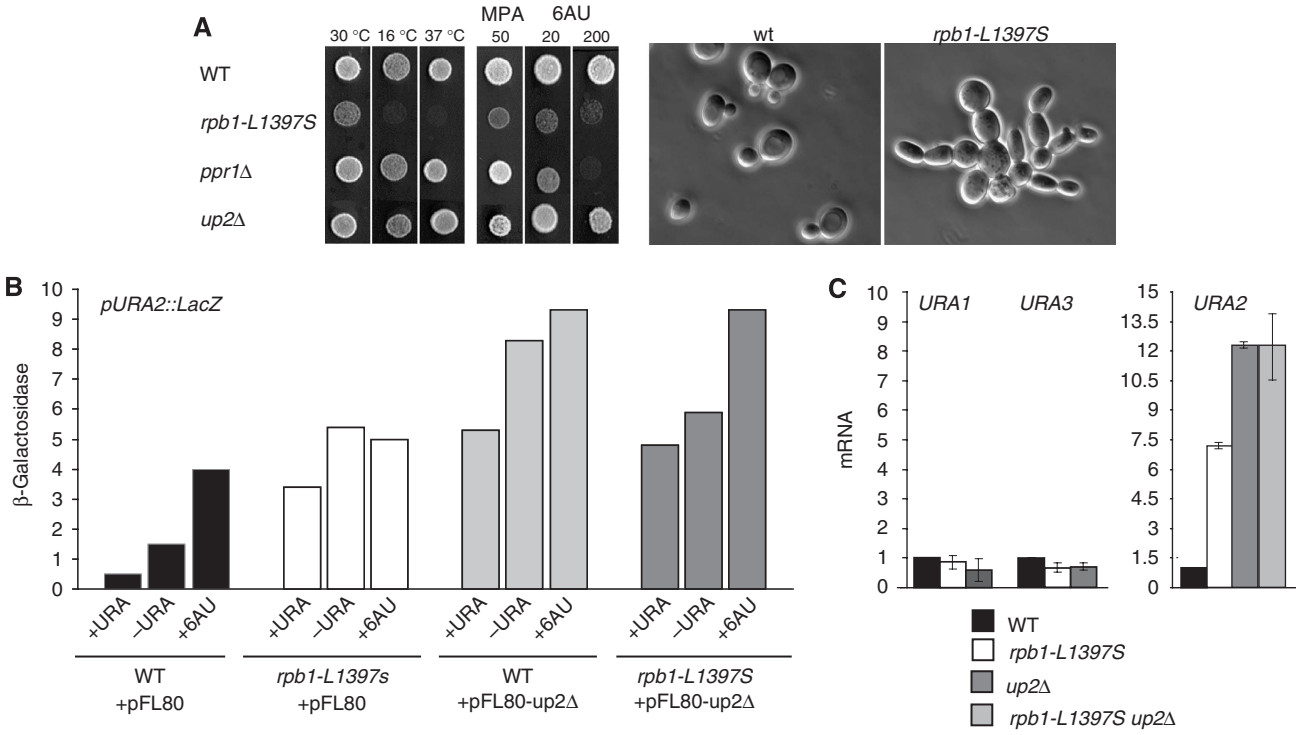

Figure 5 Properties of Switch 1 loop mutants. (**A**) GR44-11C (WT) and D711-13B (*rpb1-L1397S*) cells spotted on SD + aa or SD + aa supplemented with mycophenolate (50 mg/l) or 6-azauracil (20 and 200 mg/l). FL53 (*ppr1*Δ) and FL51 (*up2*Δ) were used as controls. Cells were microphotographed in exponential cultures grown in SD + aa at 30 °C. (**B**) Expression of *pURA2*::*LacZ*. β-galactosidase was assayed as shown in Figure 2A, in strains BMA64-URA3 (WT) and FL-M9-URA3 (*rpb1-L1397S*) transformed with the pFL80 or pFL80-up2Δ *pURA2*::*LacZ* reporter plasmids. (**C**) GR44-11C (WT) or YGH2 (WT), D711-13B (*rpb1-L1397S*), FL51 (*up2*Δ) and D876-10D (*rpb1-L1397S up2*Δ) were exponentially grown in CSM. Total RNA was extracted as described in Materials and methods. Steady-state levels of *URA1, URA2* and *URA3* mRNAs were quantified by RT–PCR and expressed in arbitrary units, where 1.0 corresponds to the wild-type level of *URA1* mRNA in CSM medium for *URA1* and *URA3*, and to the wild-type level of *URA2* mRNA in CSM.

rpb1-L1397S highly expressed *URA2* (Figure 5B and C). Moreover, an *rpb1-L1397S up2*Δ double-mutant had the same constitutive expression as *up2*Δ alone, and a *pURA2*::*LacZ* reporter bearing the *up2*Δ allele (plasmid pFL80-up2Δ) was expressed at the same level when tested in wild-type or in an *rpb1-L1397S* host strain (Figure 5B and C). In other words, *rpb1-L1397S* and *up2*Δ have epistatic effects on *URA2* expression, thus strongly suggesting that they are defective in the same mechanism downregulating *URA2* in response to uracil.

The six amino-acid segment occupied by L1397, S1401 and F1402 corresponds to Rpb1-α47b, one of the two α helices forming the Switch 1 loop domain of the RNA polymerase II active site (Gnatt *et al*, 2001). Moreover, the *rpb1-G1388V* allele, altering the Rpb1-α47a helix (Berroteran *et al*, 1994), also resulted in a high constitutive expression of *URA2* (data not shown). This high clustering was not anticipated in a UV mutagenesis, as the latter evidently affects the whole yeast genome. Our genetic screen was presumably not saturating, and we cannot exclude that *URA2* activation may, for some reason, be a general property of partly defective RNA polymerase II mutants. We thus tested the *pURA2*::*LacZ* reporter (pFL80) in 10 other slow-growing mutations partly impairing Rpb1 (*rpb1-G1437D*, *rpb1-E1351K* and *rpb1-H1367D*) or Rpb2 (*rpb2-R857K*, *rpb2-E836A*, *rpb2-D978A*, *rpb2-P1018S* and *rpb2-G1142D*) or lacking the non-essential subunits Rpb4 (*rpb4*Δ) or Rpb9 (*rpb9*Δ) (Woychik and Young, 1989; Scafe *et al*, 1990; Woychik *et al*, 1991). Except for a modest derepressing effect of *rpb2-E836A* and *rpb2-R857K*, their β-galactosidase activity was equal to or lower than the wild-type control (data not shown), thus strongly suggesting that *URA2* activation, at least to a large extent, is primarily due to changes in the Switch 1 loop.

The Switch1 loop is highly conserved in all eukaryotic and archaeal RNA polymerases (Figure 6A). Together with the α25 Bridge helix, α36 Trigger helix and the α46/47 Loop of Rpb1, it forms an identical fold in the RNA polymerase of *Sulfolobus solfataricus* (Hirata *et al*, 2008) and in yeast RNA polymerase II (Gnatt *et al*, 2001). This fold wraps the downstream end of the transcription bubble and holds the DNA template strand by the invariant R1386-E1403 Switch 1 dipole (Figure 6B and C). As discussed elsewhere (Zaros *et al*, 2007), this fold is stabilised by the C-end of the Rpb5 subunit, itself strongly conserved from archaea to eukaryotes. Bacterial RNA polymerases, on the other hand, have no Rpb5 and their Switch 1 loop is considerably extended but nevertheless adopts a very similar spatial orientation (Vassylyev *et al*, 2007).

rpb1-L1397S enhances RNA polymerase II occupancy downstream of the URA2 initiator

Consistent with the partial growth defects of *rpb1-L1397S*, a twofold reduction in RNA polymerase II occupancy was seen for *rpb1-L1397S* in single-gene ChIP assays at *ADH1* or *PYK1* (Figure 7A). This extended to the whole genome, with an average occupancy level of 62% ($R^2 = 0.80$) relatively to wild

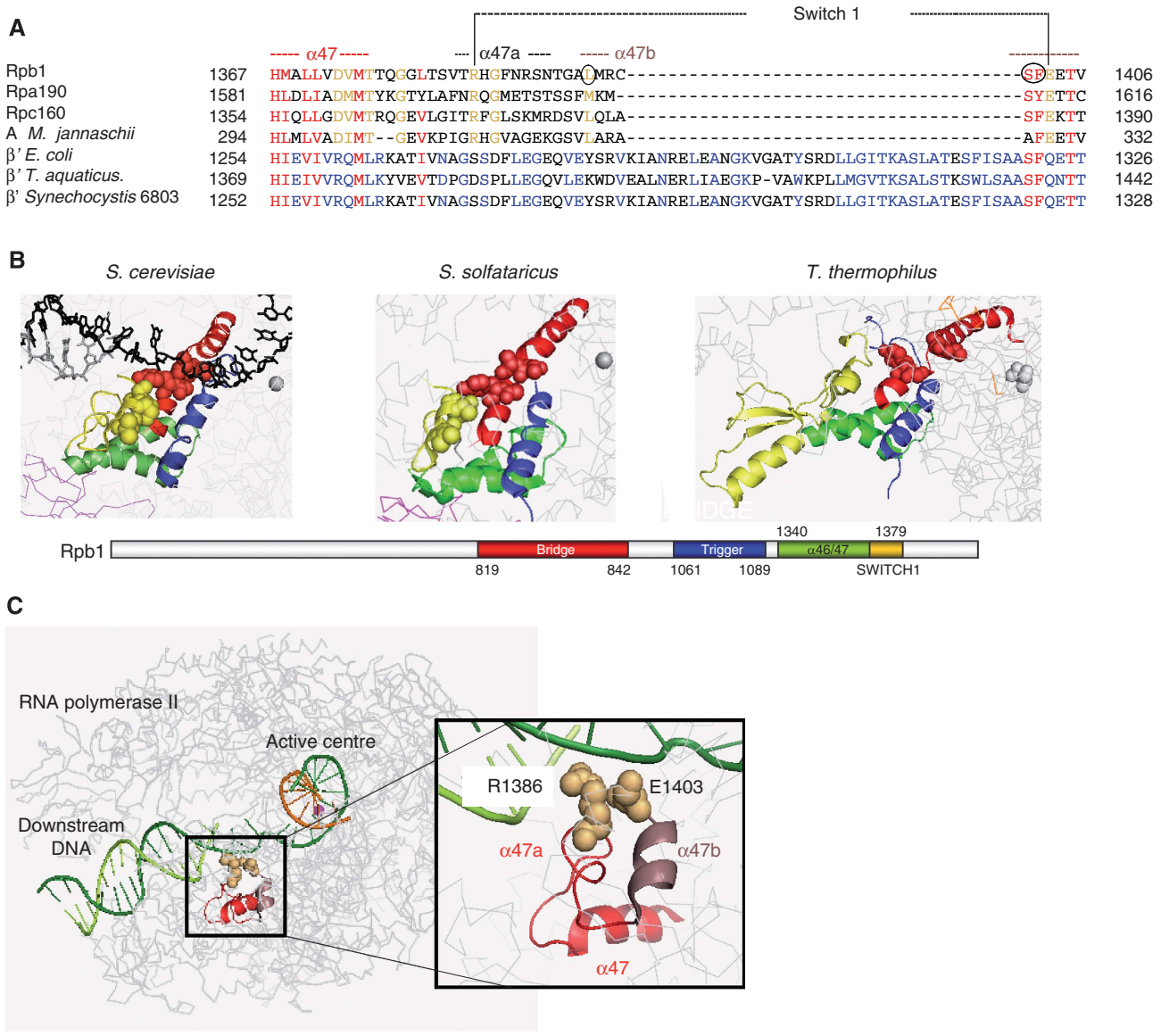

Figure 6 Organisation of the Switch 1 loop in RNA polymerase II. (**A**) Sequence alignments with yeast, archaeal and bacterial subunits. The Switch 1 loop domains (Gnatt *et al*, 2001) of Rpb1, Rpa190 and Rpc160 (*S. cerevisiae*) were aligned with the corresponding region of *M. jannaschii* (subunit A) and of the β′ subunits of *E. coli*, *Thermus aquaticus* and *Synechocystis* 6803. Amino-acid conservation is shown in red (all species), gold (Eukaryotes and Archaea) and blue (Prokaryotes only). Circles denote the mutated amino acids of *rpb1-G1388V*, *rpb1-L1397S*, *rpb1-S1401P* and *rpb1-F1402L*. (**B**) Spatial organisation of the Bridge, Trigger and Switch 1 fold in *S. cerevisiae*, *S. solfataricus* and *T. thermophilus* on the basis of PDB files 2NVZ, 2PMZ and 205I, respectively. These domains are shown on the Rpb1 sequence, with the same colour code and with numbers indicating the corresponding amino-acid positions. (**C**) Organisation of the Switch 1 loop in RNA polymerase II, using a different orientation, and showing the whole 10-subunit structure of RNA polymerase II (without Rpb4 and Rpb7). The template and non-template DNA strands and the nascent RNA are in dark green, light green and orange, respectively. A box shows the details of Switch 1 loop, underscoring the DNA-binding positions R1386 and E1403 by space-filling.

type (Figure 7B). As expected, RNA polymerase II occupancy was increased on the *URA2* open reading frame. Moreover, this increased occupancy was only seen downstream of the *URA2* initiator region (Figure 7C). Similar results were obtained in ChIP assays done in *RPB3*::*3HA rpb1-L1397S* cells, showing that this effect is independent of the precipitating antigen (Figure 7D). In contrast, two RNA polymerase II alleles (*rpb2-P1018S* and *rpb9*Δ) with partial growth defects similar to those of *rpb1-L1397S* significantly reduced RNA polymerase II signal, upstream and downstream of the initiator region. Taken together, these data clearly show that *rpb1-L1397S* activates *URA2* by extending RNA polymerase II occupancy downstream of the initiator region, thus recapitulating the effect seen above for *up2*Δ or for wild-type and *ppr1*Δ cells exposed to 6-azauracil.

rpb1-L1397S extends RNA polymerase II downstream of IMD2, IMD3 and URA8

We have seen above that *rpb1-L1397S* generally reduced RNA polymerase II occupancy, except for *URA2*. This was also consistent with genome-wide transcriptome assays, showing a moderate but significant overexpression of *URA2* in *rpb1-L1397S*, compared with an isogenic wild-type control (Figure 8A). Furthermore, these transcriptome and genome-

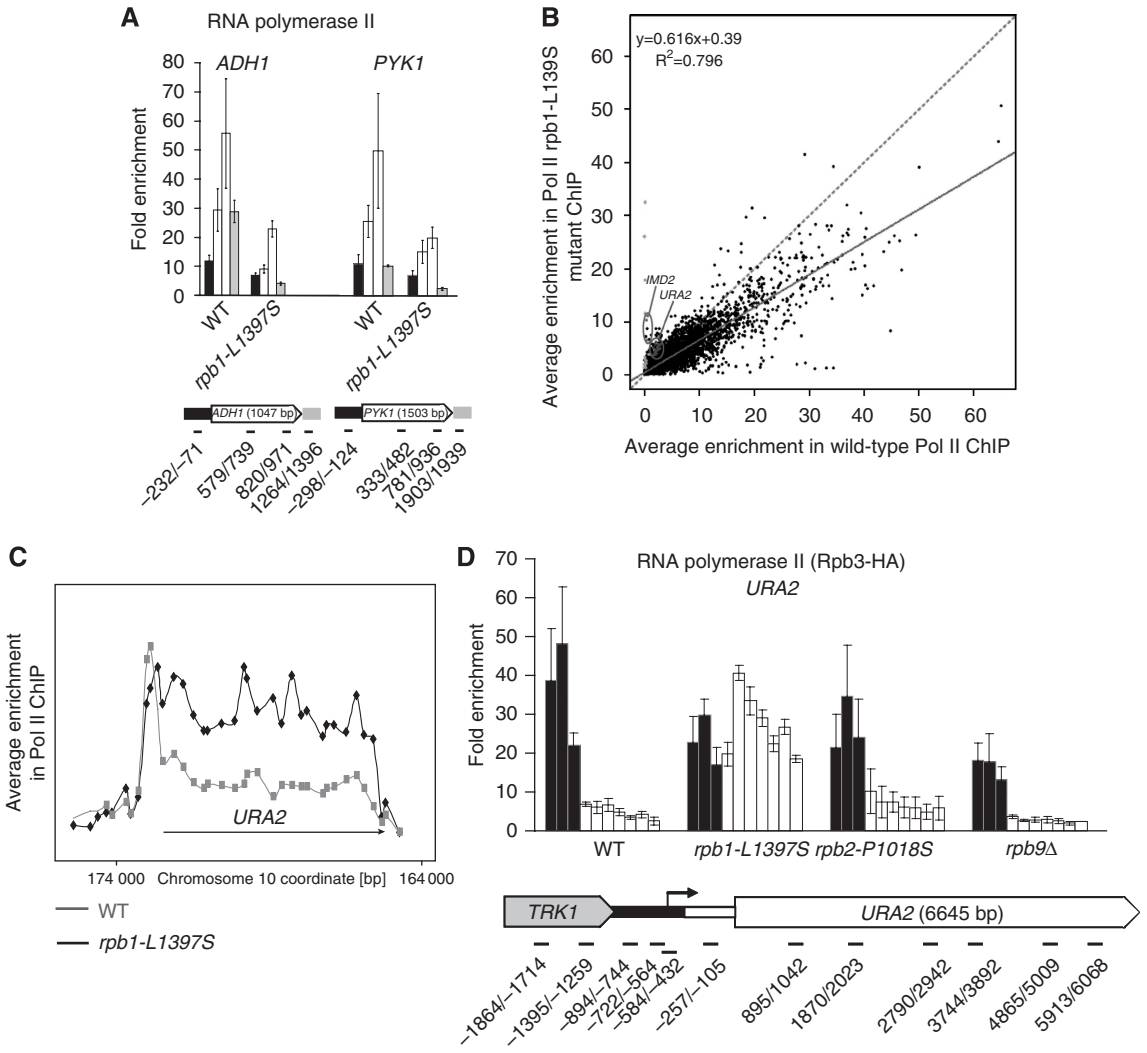

Figure 7 RNA polymerase II occupancy in *rpb1-L1397S*. (**A**) RNA polymerase II occupancy at *ADH1* and *PYK1* in D535-4D (*RPB3*::*HA*) and D535-9D (*rpb1-L1397S RPB3*::*HA*). Cells were grown in SD + aa at 30 °C. RNA polymerase II was immunoprecipitated with anti-HA antibodies. A schematic map represents the oligonucleotide pairs used as primers. Position +1 corresponds to the initiator ATG. (**B**) Genome-wide ChIP assays. Three independent cultures of YGH2 (wild-type) and D711-13B (*rpb1-L1397S*) were grown in YPD at 30 °C. Chromatin was extracted and analysed as described previously (Ghavi-Helm *et al*, 2008). (**C**) Distribution of RNA polymerase II at the *URA2* locus. Data were extracted from genome-wide analysis shown in Figure 7B above. The wild-type and *rpb1-L1397S* profiles are shown in grey and black, respectively. (**D**) Effect of *rpb1-L1397S*, *rpb2-P1018S* and *rpb9*Δ on RNA polymerase II occupancy at *URA2*. Experimental conditions were as shown in Figure 7A. The strains used were D535-4D (*RPB3*::*HA*), D535-9D (*rpb1-L1397S RPB3*::*HA*), YMW304-8C (*rpb2-P1018S RPB3*::*HA*) and YWM305-2D (*rpb9*Δ *RPB3*::*HA*).

wide RNA polymerase II occupancy assays identified two other genes, *IMD2* (IMP dehydrogenase) and *URA8* (CTP synthase), which were both overexpressed and over-occupied by RNA polymerase II in *rpb1-L1397S*. A few additional genes were also overexpressed in the *rpb1-L1397S* transcriptome, but with no higher RNA polymerase II occupancy of their open reading frames (data not shown). Conversely, *rpb1-L1397S* enhanced RNA polymerase II at *ADE12* (adenylosuccinate synthase), but had no detectable effect on its mRNA level.

Saccharomyces cerevisiae has two CTP synthases (*URA7* and *URA8*) and three active IMP dehydrogenase genes (*IMD2*, *IMD3* and *IMD4*), with *IMD1* as a pseudo-gene inactivated by a frame-shift mutation in most laboratory strains (Ozier-Kalogeropoulos *et al*, 1994; Nadkarni *et al*, 1995; Hyle *et al*, 2003). *URA7* and *URA8* are sufficiently different to be distinguished by individual RT–PCR assays, which clearly showed that *rpb1-L1397S* activated only *URA8* (Figure 8B). RT–PCR assays also confirmed the overexpression of the IMP dehydrogenase mRNA in *rpb1-L1397S* but did not clearly distinguish between *IMD2*, *IMD3* and *IMD4*, due to their very similar nucleotide sequences. However, our genome-wide ChIP assays readily discriminated between these three genes. This revealed that *rpb1-L1397S* strongly activated *IMD2*, with some effect on *IMD3* (Figure 8C) and no effect at all on *IMD4* (not shown). We considered the possibility that the activation of CTP synthase and IMP dehydrogenase genes may be an indirect effect of *URA2* overexpression, reflecting an increased cellular pool of UTP. However, the activation of *URA2* in *up2*Δ was not accompanied by a parallel increase in *URA8* or IMP dehydrogenase mRNA, thus strongly arguing for a direct activating effect of *rpb1-L1397S* (Figure 8B).

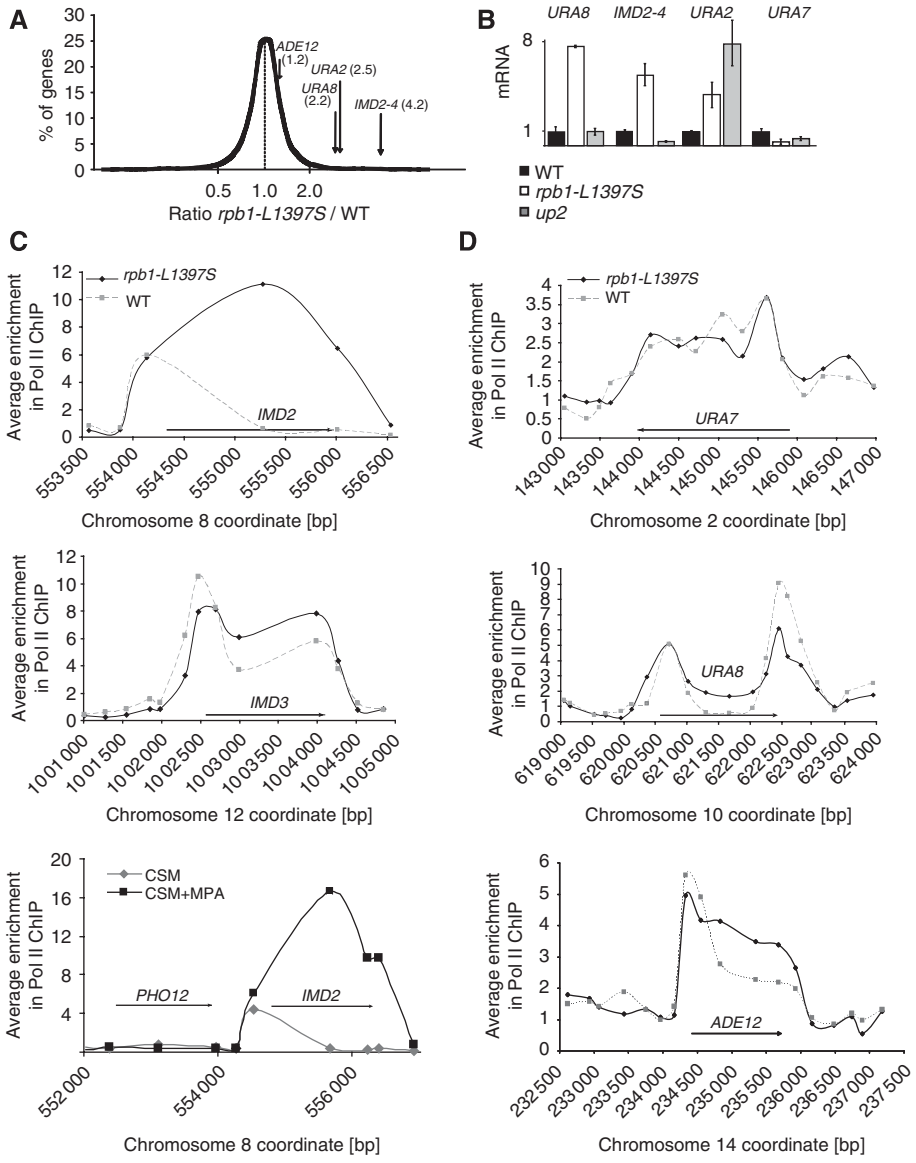

Figure 8 Effect of *rpb1-1397S* on *IMD2*, *IMD3*, *ADE12*, *URA7* and *URA8*. (**A**) Enrichment of RNA polymerase II transcripts in D535-9D (*rpb1-L1397S*) compared with an isogenic wild-type obtained by complementation with pFL36-RPB1. The histogram represents median percentile ranks of Cy3/Cy5 fluorescence ratios. Data are based on three independent cultures of each strain. The *URA2*, *URA8*, *ADE12* and *IMD2-4* transcripts are individualised by arrows. (**B**) RT–PCR of individual mRNAs. GR44-11C (WT), D711-13B (*rpb1-L1397S*) and FL51 (*up2*Δ) were exponentially grown in SD + aa. Total RNA was extracted as described in Materials and methods. Individual mRNAs were quantified by RT–PCR and expressed in arbitrary units, where 1.0 corresponds to the wild-type level. (**C**) RNA polymerase II occupancy at *IMD2* and *IMD3*. Data were extracted from the genome-wide analysis shown above (Figure 7B) except for *IMD2* in wild-type cells grown in CSM + MPA, taken from Ghavi-Helm *et al* (2008). (**D**) RNA polymerase II occupancy at *URA7*, *URA8* and *ADE12*. Data were extracted from the genome-wide analysis shown above (Figure 7B).

Previous studies have shown that *IMD2* is controlled by an initiation switch between short transcripts, synthesised from an upstream initiator, and full-length mRNAs starting from a downstream initiator (Escobar-Henriques *et al*, 2003; Steinmetz *et al*, 2006; Kopcewicz *et al*, 2007; Jenks *et al*, 2008). RNA polymerase II is confined to the upstream initiator when wild-type cells are grown under repressing conditions (Steinmetz *et al*, 2006), but extended to the entire *IMD2* gene in *rpb1-L1397S* or in derepressed wild-type cells that have been exposed to mycophenolate (Figure 8C). In *URA8* and perhaps in *ADE12*, Thiebaut *et al* (2008) have provided evidence for a transcriptional switch reminiscent of the *IMD2* case. Again, RNA polymerase II was mostly restricted to the upstream part of the gene in wild-type cells grown under repressing conditions, but extended to the entire *URA8* open reading frame in *rpb1-L1397S* (Figure 8C). A similar effect may apply to *ADE12*, encoding the first step of the ATP biosynthetic pathway, where *rpb1-L1397S* moderately increased RNA polymerase II occupancy downstream of the promoter region (Figure 8D).

Discussion

Previous studies have shown that *URA1* or *URA3* are specifically activated by Ppr1, a Zn activator of the Gal4-type which responds to increased concentration of the orotate and/or dihydro-orotate precursors of UTP (Loison *et al*, 1980; Losson and Lacroute, 1981; Flynn and Reece, 1999).

This leads to an increased RNA polymerase II occupancy at the *URA1* and *URA3* promoters, lost in the *ppr1*Δ-null allele, indicating a 'classical' mode of gene-specific activation on the basis of a more effective recruitment of RNA polymerase II by its pre-initiation complex. *URA2*, which encodes the main rate-limiting enzyme of UTP biosynthesis, is activated when UTP is depleted by 6-azauracil addition. However, the *ppr1*Δ-null allele is fully competent for *URA2* transcription. Moreover, and in contrast to *URA1* or *URA3*, *URA2* activation does not change the amount of RNA polymerase II residing at or upstream of the *URA2* initiator region, but operates instead by extending RNA polymerase II occupancy to the *URA2* open reading frame.

Three *cis*-acting mutations constitutively expressing *URA2* were selected in this study. They corresponded to very similar deletions (*up2*Δ, *up6*Δ and *up10*Δ) removing a 55–70 nt DNA region upstream of the *URA2* initiator. The *up2*Δ mutation was studied in more detail. It extended RNA polymerase II to the entire *URA2* open reading frame, with no change in the RNA polymerase II signal upstream of the *URA2* initiator, thus recapitulating the pattern seen in UTP-depleted wild-type or *ppr1*Δ cells. Further studies (Thiebaut *et al*, 2008) have shown that the corresponding DNA is transcribed from an initiator region located some 100 nt upstream of the main *URA2* mRNA 5′-ends identified here, producing unstable RNAs with the same transcriptional orientation as *URA2*, which were no longer detected in *up2*Δ. Taken together, these data suggest that *URA2* may be regulated by an attenuation mechanism related to the one recently described for *IMD2* (Escobar-Henriques *et al*, 2003; Davis and Ares, 2006; Steinmetz *et al*, 2006; Kopcewicz *et al*, 2007; Jenks *et al*, 2008).

A genome-wide selection for *trans*-acting mutations constitutively expressing *URA2* yielded three tightly clustered *rpb1* mutations (*rpb1-L1397S*, *rpb1-S1401P* and *rpb1-F1402L*), corresponding to the Rpb1α-47b helix of the Switch 1 loop. *rpb1-G1388V*, which was initially selected for its ability to alter transcription initiation in favour of downstream sites (Berroteran *et al*, 1994) and belongs to the Rpb1-α47a helix, also activates *URA2* (see also Thiebaut *et al*, 2008). In contrast, other partly defective RNA polymerase II mutations failed to derepress *URA2*, indicating that *URA2* activation is by no means a general property of RNA polymerase II mutants. Similar to *up2*Δ, *rpb1-L1397S* activates *URA2* by extending RNA polymerase II occupancy to the entire open reading frame, with no change in the signal upstream of the *URA2* initiator, thereby reproducing the effect seen in *up2*Δ and in UTP-depleted wild-type cells. Moreover, *up2*Δ and *rpb1-L1397S* had epistatic effects on *URA2* expression, indicating that *rpb1-L1397S* is defective in the attenuation mechanism lost in *up2*Δ itself. Finally, *rpb1-L1397S* and wild-type *URA2* mRNAs had similar 5′-ends, as determined by 5′-RACE assays, and therefore use the same transcription initiator.

The above-mentioned data indicate that changes in the Switch 1 loop specifically activate *URA2*, despite their adverse effects on growth and their reduced genome-wide RNA polymerase II occupancy. Moreover, we were unable to identify mutants encoding a specific regulator of *URA2*, although it remained possible that such mutants are lethal because they perturb some essential cellular process. The Switch 1 loop forms an invariant R1386(α47a)-E1403(α47b) dipole, holding the DNA template strand at positions +2/+3 downstream of the catalytic Mg^{2+} (Gnatt *et al*, 2001). This domain is highly conserved among eukaryotic and archaeal RNA polymerases (Cramer *et al*, 2001; Hirata *et al*, 2008) and a related structure exists in the bacterial enzyme, where it also binds DNA at positions +2/+3 downstream of the catalytic Mg^{2+} (Vassylyev *et al*, 2007; Zaros *et al*, 2007).

The relation of this domain to the entry route of NTPs in RNA polymerase II is unclear (Landick, 2005). One possibility is that NTPs reach the catalytic site of RNA polymerase II by its funnel-shaped pore (Cramer *et al*, 2001; Kettenberger *et al*, 2003; Westover *et al*, 2004; Landick, 2005), but it has also been suggested that NTPs enter through the large DNA channel, transiently binding the DNA template at nucleotides +2, +3 and possibly +4 (Gong *et al*, 2005), which implies that NTPs pass by the Switch 1 loop before reaching the catalytic Mg^{2+}. Hence, the Switch 1 loop may act as an NTP-sensing module, enabling RNA polymerase II to adopt a processive mode of elongation when enough NTP is available. This would optimise the efficiency of transcription, which may account for the cold- and heat-sensitive defects of *rpb1-L1397S*, *rpb1-S1401P* and *rpb1-F1402L* and their increased sensitivity to 6-azauracil and mycophenolate.

Strikingly, *rpb1-L1397S* also extended RNA polymerase II occupancy downstream of the *IMD2/IMD3* (IMP dehydrogenase) and *URA8* (CTP synthase) promoters, with some evidence for a similar effect on *ADE12* (adenylosuccinate synthase). This makes biological sense, as the corresponding genes encode rate-limiting enzymes in the *de novo* synthesis of GTP, CTP and ATP. This suggests the rather non-canonical view that nucleoside triphosphate shortage or RNA polymerase II Switch 1 loop mutations (assumed here to mimic that shortage) specifically activate the expression of genes that are themselves critical for the *de novo* synthesis of NTPs. In other words, the transcriptional response to NTP shortage would not rely on dedicated activators or repressors (which have been vainly searched for in the case of *URA2* and *IMD2*) but would be mediated by an NTP-sensing mechanism built in the structure of RNA polymerase II itself.

In *IMD2*, there is good evidence that RNA polymerase II molecules are recruited on a common pre-initiation complex, followed by a start site switch leading to the alternative production of upstream transcripts ended by Nab3/Nrd1-dependent termination or full-length mRNAs transcribed from a downstream initiator region. Start site selection is presumably dictated by the nucleotide composition of the surrounding DNA, with upstream transcription starting at Gs, whereas *IMD2* transcription starts in a G-poor DNA region and is therefore favoured by low GTP pools (Escobar-Henriques *et al*, 2003; Davis and Ares, 2006; Steinmetz *et al*, 2006; Kopcewicz *et al*, 2007; Jenks *et al*, 2008). The *URA2* start choice, however, depends on a different mechanism, as upstream initiation does not occur preferentially at T's and is not sensitive to the abundance of uracil (Thiebaut *et al*, 2008). Conversely, we found that 3 out of 10 *URA2* cDNAs produced under activating conditions started with a T, which argues against the simple idea of a selection driven by the nature of the starting nucleotide. Nevertheless, the upstream initiator is followed by an ~60 nt T-rich domain, continued by 40 nt that are conspicuously poor in T's and harbour the *URA2* mRNA 5′-ends. This pattern is conserved among all *Saccharomyces* species sequenced to data (see

Supplementary data), and we would be surprised if it did not provide some form of UTP-sensing. Further studies are clearly needed to better understand how RNA polymerase II responds to NTP shortage, and how this response is ultimately converted into a specific control of the *IMD2*, *URA2* and *URA8* genes.

Materials and methods

Plasmids

Newly constructed plasmids are listed in Supplementary data. Plasmids pFL35-II, pFL36-CII (*CEN6 LEU2*) and pFL39-CII (*CEN6 TRP1*), corresponding to pFL35, pFL36 and pFL39 (Bonneaud *et al*, 1991), with an extended polylinker of 90 nucleotides (Supplementary data). pFL80 and pFL82 are *pURA2*::*LacZ pURA2* reporters derived from pFL39-CII and pFL36-CII, respectively. They harbour a *Kpn*I–*Bam*HI–*Not*I *pURA2*::*LacZ* cassette of 4392 nt. The *Kpn*I–*Bam*HI segment (1254 nt) is formed by the *TRK1–URA2* intergenic region, preceded by *GGTACC*AGCACAACGCTCTAA (the *Kpn*I site is in italics) and followed by AT*GGATCC* (*Bam*HI). It is cloned in-frame to the initiator ATG of a *Bam*HI–*Not*I *LacZ* cassette. pFL83 is pFL80 where the *LacZ* open reading frame has been replaced by a *Bam*HI–*Not*I *HIS3* (*S. cerevisiae*) cassette. As pFL80 poorly complemented *trp1* mutant strains, which overexpressed the *pURA2* promoter (due to some transcriptional interference between *LacZ* and *TRP1*), we also used pFL80-H2, a *pURA2*::*LacZ* reporter with a lower *LacZ* expression. This plasmid was selected after random insertion of genomic *Hin*dIII fragments in the unique *Hin*dIII site downstream of *LacZ* (Supplementary data). The *Hin*dIII fragment of pFL80-H2 corresponded to positions 7679–8251 of the *TEL1* gene and was inserted in a transcriptional orientation opposite to the one of *TRP1*.

Plasmids pFL80-KB, pFL80-BS and pFL80-CS correspond to *Kpn*I/*Bsr*GI, *Bsr*GI/*Sal*I and *Cla*I/*Sal*I deletions of pFL80, respectively. pFL80-INTΔ was precisely deleted of the DNA comprised between nucleotides −384 to −63, where 1 corresponds to the *URA2* start codon. The pFL83-upΔ2, -up6Δ and -up10Δ plasmids were obtained by error-prone amplification of the *Kpn*I–*Bam*HI cassette of pFL83, which was recombined into the original vector by co-transformation with linearised pFL83 DNA deleted of its *Bsr*GI–*Sal*I fragment. Mutant plasmids were selected on 3-aminotriazol in the presence of uracil, amplified in *Escherichia coli*, retransformed and verified for their overexpression. The corresponding *up*Δ alleles were transferred to pFL80 by *Kpn*I–*Bam*HI subcloning.

Yeast strains

Yeast mutants are listed as Supplementary data. Plasmid shuffle assays were done in the presence of 5-fluoro-orotic acid to counter-select *URA3* plasmids (Boeke *et al*, 1984). Except when stated otherwise, they were constructed in BMA64-1A and BMA64-URA3, a *URA3*$^{+}$ revertant of BMA64-1A (Baudin-Baillieu *et al*, 1997). Yeasts were grown on SD + aa, corresponding to the standard synthetic dextrose medium supplemented with histidine, tryptophan and adenine sulphate (20 mg/l), leucine and lysine (30 mg/l). In β-galactosidase assays, SD + aa was replaced by the complete synthetic medium CSM (manufactured by BIO101) supplemented with a complete set of amino acids but lacking uracil. CSM supplemented with 2 g/l of uracil (CSM + U) fully represses *URA2*, whereas adding 6-azauracil at 20 mg/l (CSM + 6AU) fully activates *URA2*.

FL50 was obtained by inserting the integrative plasmid pFL81 (*TRP1 pURA2*::*HIS3*) at the *Eco*RV site of the *trp1-1* allele in W303-1B. When grown in the presence of uracil, this strain has an increased sensitivity to 3-aminotriazol, due to the repression of its *pURA2*::*HIS3* reporter. FL52 is FL50 transformed with pFL82 (*LEU2 pURA2*::*LacZ*). FL-M9, M10, M13 and M23 are FL52 mutants selected from UV-irradiated cells (about 1% survival) plated for 3 days at about 4×10^6 cells on leucine omission plates with uracil (2 g/l) and 50 or 100 mM of 3-aminotriazol. β-galactosidase was assayed in a loop of cells put on Whatman paper soaked in 2 ml of Z buffer (Miller, 1972) containing X-Gal (1 g/l) and a drop of zymolase. Dark blue clones were tested again, using freshly grown cells suspended in 0.6 ml of Z buffer and vortexed for 1 min with an equal volume of glass beads. Cells were refrigerated in an ice bath, treated with a second round of glass bead extraction, pelleted by centrifugation at 14 000 r.p.m. and tested for β-galactosidase after 10 min at 37 °C. Mutant strains with an at least fivefold increase in β-galactosidase were retained for further analysis. A fifth mutant was a *fur1* allele partly defective for UMP pyrophosphorylase, impairing the metabolic conversion of uracil into UMP.

FL51, with the *up2*Δ allele integrated on the chromosome by homologous recombination, was constructed by subcloning the *Kpn*I–*Bam*HI fragment of pFL81-up2Δ into pFL35-II. The resulting plasmid was linearised at the *Bsm*I site of the *pURA2* promoter region, to direct its integration by homologous recombination with the *pURA2* region of BMA64-URA3. The corresponding transformants harboured the *TRP1* cassette flanked by wild-type and *up2*Δ tandem copies of *pURA2*. Tryptophan auxotrophic clones spontaneously occurred by recombination between these *pURA2* copies and were selected by nystatin enrichment (Snow, 1966), yielding single copies of *pURA2*. Among them, *up2*Δ mutants were identified by their weak resistance to 5-fluorouracil (10^{-5} M), and were further checked by PCR amplification.

ChIP and genome-wide ChIP-chip assays

Chromatin immunoprecipitation assays were as described elsewhere (Ghavi-Helm *et al*, 2008). All experiments were performed on three independent cultures of 100 ml, harvested at an OD_{600} of 0.3–0.5. Cells were grown in SD + aa with or without uracil, or UTP-depleted by adding 200 mg/l of 6-azauracil to log-phase cells grown in SD + aa and grown for three additional doubling times. RNA polymerase II was immunoprecipitated with Dynabeads anti-mouse IgG (Dynal Biotech), using anti-CTD antibodies (8WG16), or anti-hemagglutinin A antibodies (12CA5) in the case of Rpb3-HA tagged strains. Sua7-TAP and Rad3-TAP proteins were directly immunoprecipitated on Dynabeads anti-mouse IgG. Phosphorylated variants of the RNA polymerase CTD domain were immunoprecipitated with Dynabeads anti-mouse IgM, using anti-Ser2^{P} (H5, Covance) and anti-Ser5^{P} (H14, Covance) antibodies. ChIP signals were calculated by the immunoprecipitation/input signal. The value 1.0 was arbitrarily given to the reference signal provided by amplifying the *GAL1* gene. Genome-wide ChIP assays, on the basis of three independent cultures in YPD or CSM medium for mycophenolate experiments (10 mg/l) medium, were described elsewhere (Harismendy *et al*, 2003) and were based on DNA arrays with over 40 000 oligonucleotide probes covering 12 Mb of the yeast genome (Ghavi-Helm *et al*, 2008).

RNA and transcriptome assays

Total RNA was extracted from three independent, exponential cultures with hot phenol and reverse-transcribed using 1 μg of total RNA, Super-Script II reverse transcriptase (Invitrogen) and random hexamers as primers. Controls without reverse transcriptase showed negligible levels of DNA contamination. DNA was quantified by real-time PCR amplification (Applied Biosytems, System SDS Software) using primers listed in Supplementary data. mRNA levels are calculated as a ratio of measured mRNA and *ACT1* mRNA. The 5′-ends of *URA2* mRNAs were mapped by sequencing cDNAs obtained by the RNA ligase mediated-RACE technique (using an RLM-RACE kit from Ambion), according to the protocol provided by the manufacturer. Yeast micro-arrays were probed against total RNA extracted from three independent cultures of strains BMA64-URA3 (wild type) and FL-M9 (*rpb1-L1397S*) grown on SD + aa at 30 °C, to an OD_{600} of 0.55. cDNA synthesis, purification, indirect labelling, microarray hybridisation, scanning and analysis were done according to standard protocols (Soutourina *et al*, 2006), with two independent hybridisations for each RNA batch.

Supplementary data

Supplementary data are available at *The EMBO Journal* Online (http://www.embojournal.org).

Acknowledgements

We thank Fred Beckouët, Antonin Morillon, Bertand Séraphin and Michel Werner for strains, plasmids and helpful discussions. We are especially thankful to Alain Jacquier and Domenico Libri for communicating unpublished data before publication. This work was partly funded by the Ligue pour la Recherche sur le Cancer (FL). DD and MK benefited from fellowships of the French Association pour la Recherche sur le Cancer and Fondation pour la Recherche Médicale.

References

Arigo JT, Carroll KL, Ames JM, Corden JL (2006) Regulation of yeast NRD1 expression by premature transcription termination. *Mol Cell* **21:** 641–651

Baudin-Baillieu A, Guillemet E, Cullin C, Lacroute F (1997) Construction of a yeast strain deleted for the TRP1 promoter and coding region that enhances the efficiency of the polymerase chain reaction-disruption method. *Yeast* **13:** 353–356

Berroteran RW, Ware DE, Hampsey M (1994) The sua8 suppressors of *Saccharomyces cerevisiae* encode replacements of conserved residues within the largest subunit of RNA polymerase II and affect transcription start site selection similarly to sua7 (TFIIB) suppressors. *Mol Cell Biol* **14:** 226–237

Boeke JD, Lacroute F, Fink GR (1984) A positive selection for mutants lacking orotidine-5′-phosphate decarboxylase activity in yeast: 5-fluoro-orotic acid resistance. *Mol Gen Genet* **197:** 345–346

Bonneaud N, Ozier-Kalogeropoulos O, Li G, Labouesse M, Minvielle-Sebastia L, Lacroute F (1991) A family of low and high copy replicative, integrative and single-stranded *S. cerevisiae/E. coli* shuttle vectors. *Yeast* **7:** 609–615

Cramer P, Bushnell DA, Kornberg RD (2001) Structural basis of transcription: RNA polymerase at 2.8 Å resolution. *Science* **292:** 1863–1876

Davis CA, Ares Jr M (2006) Accumulation of unstable promoter-associated transcripts upon loss of the nuclear exosome subunit Rrp6p in *Saccharomyces cerevisiae*. *Proc Natl Acad Sci USA* **103:** 3262–3267

Escobar-Henriques M, Daignan-Fornier B, Collart MA (2003) The critical cis-acting element required for IMD2 feedback regulation by GDP is a TATA box located 202 nucleotides upstream of the transcription start site. *Mol Cell Biol* **23:** 6267–6278

Exinger F, Lacroute F (1992) 6-Azauracil inhibition of GTP biosynthesis in *Saccharomyces cerevisiae*. *Curr Genet* **22:** 9–11

Flynn PJ, Reece RJ (1999) Activation of transcription by metabolic intermediates of the pyrimidine biosynthetic pathway. *Mol Cell Biol* **19:** 882–888

Ghavi-Helm Y, Michaut M, Acker J, Aude J, Thuriaux P, Werner M, Soutourina J (2008) Genome-wide location analysis revealed a role for TFIIS in RNA polymerase III transcription. *Genes Dev* **14:** 1934–1947

Gnatt AL, Cramer P, Fu J, Bushnell DA, Kornberg RD (2001) Structural basis of transcription: an RNA polymerase elongation complex at 3.3 Å resolution. *Science* **292:** 1876–1882

Gong XQ, Zhang C, Feig M, Burton ZF (2005) Dynamic error correction and regulation of downstream bubble opening by human RNA polymerase II. *Mol Cell* **18:** 461–470

Harismendy O, Gendrel CG, Soularue P, Gidrol X, Sentenac A, Werner M, Lefebvre O (2003) Genome-wide location of yeast RNA polymerase III transcription machinery. *EMBO J* **22: 4738–4747**

Hirata A, Klein BJ, Murakami KS (2008) The X-ray crystal structure of RNA polymerase from Archaea. *Nature* **451:** 851–854

Hyle JW, Shaw RJ, Reines D (2003) Functional distinctions between IMP dehydrogenase genes in providing mycophenolate resistance and guanine prototrophy to yeast. *J Biol Chem* **278:** 28470–28478

Jenks MH, O'Rourke TW, Reines D (2008) Properties of an intergenic terminator and start site switch that regulate IMD2 transcription in yeast. *Mol Cell Biol* **28:** 3883–3893

Juneau K, Palm C, Miranda M, Davis RW (2007) High-density yeast-tiling array reveals previously undiscovered introns and extensive regulation of meiotic splicing. *Proc Natl Acad Sci USA* **104:** 1522–1527

Kettenberger H, Armache KJ, Cramer P (2003) Architecture of the RNA polymerase II-TFIIS complex and implications for mRNA cleavage. *Cell* **114:** 347–357

Kopcewicz KA, O'Rourke TW, Reines D (2007) Metabolic regulation of IMD2 transcription and an unusual DNA element that generates short transcripts. *Mol Cell Biol* **27:** 2821–2829

Lacroute F, Piérard A, Grenson M, Wiame JM (1965) The biosynthesis of carbamoylphosphate in *Saccharomyces cerevisiae*. *J Gen Microbiol* **40:** 127–142

Landick R (2005) NTP-entry routes in multi-subunit RNA polymerases. *Trends Biochem Sci* **30:** 651–654

Loison G, Losson R, Lacroute F (1980) Constitutive mutants for orotidine 5′-phosphate decarboxylase and dihydroorotic acid dehydrogenase in *Saccharomyces cerevisiae*. *Curr Genet* **2:** 39–44

Losson R, Lacroute F (1981) Cloning of a eukaryotic regulatory gene. *Mol Gen Genet* **184:** 394–399

Miller JH (1972) *Experiments in Molecular Genetics*. Cold Spring Harbor: Cold Spring Harbor Laboratory Press. pp 352–353

Nadkarni AK, McDonough VM, Yang WL, Stukey JE, Ozier-Kalogeropoulos O, Carman GM (1995) Differential biochemical regulation of the URA7- and URA8-encoded CTP synthetases from *Saccharomyces cerevisiae*. *J Biol Chem* **270:** 24982–24988

Ozier-Kalogeropoulos O, Adeline MT, Yang WL, Carman GM, Lacroute F (1994) Use of synthetic lethal mutants to clone and characterize a novel CTP synthetase gene in *Saccharomyces cerevisiae*. *Mol Gen Genet* **242:** 431–439

Potier S, Lacroute F, Hubert JC, Souciet JL (1990) Studies on transcription of the yeast URA2 gene. *FEMS Microbiol Lett* **60:** 215–219

Potier S, Souciet J-L, Lacroute F (1987) Correlation between restriction map, genetic map and catalytic functions in the gene complex URA2. *Mol Gen Genet* **209:** 283–289

Rothstein R (1991) Targeting, disruption, replacement, and allele rescue: integrative DNA transformation in yeast. *Methods Enzymol* **194:** 281–301

Scafe C, Martin C, Nonet M, S P, Okamura S, Young RA (1990) Conditional mutations occur predominantly in highly conserved residues of RNA polymerase II subunits. *Mol Cell Biol* **10:** 1270–1275

Serre V, Penverne B, Souciet JL, Potier S, Guy H, Evans D, Vicart P, Herve G (2004) Integrated allosteric regulation in the *S. cerevisiae* carbamylphosphate synthetase—aspartate transcarbamylase multifunctional protein. *BMC Biochem* **5:** 6

Shaw RJ, Wilson JL, Smith KT, Reines D (2001) Regulation of an IMP dehydrogenase gene and its overexpression in drug-sensitive transcription elongation mutants of yeast. *J Biol Chem* **276:** 32905–32916

Snow R (1966) An enrichment method for auxotrophic yeast mutants using the antibiotic 'nystatin'. *Nature* **211:** 206–207

Soutourina J, Bordas-Le Floch V, Gendrel G, Flores A, Ducrot C, Dumay-Odelot H, Soularue P, Navarro F, Cairns BR, Lefebvre O, Werner M (2006) Rsc4 connects the chromatin remodeler RSC to RNA polymerases. *Mol Cell Biol* **26:** 4920–4933

Steinmetz EJ, Warren CL, Kuehner JN, Panbehi B, Ansari AZ, Brow DA (2006) Genome-wide distribution of yeast RNA polymerase II and its control by Sen1 helicase. *Mol Cell* **24:** 735–746

Thiebaut M, Colin J, Neil H, Jacquier A, Seraphin B, Lacroute F, Libri D (2008) Futile cyle of transcription initiation and termination modulates the response to nucleotide shortage in *S. cerevisiae*. *Mol Cell* (in press)

Thiebaut M, Kisseleva-Romanova E, Rougemaille M, Boulay J, Libri D (2006) Transcription termination and nuclear degradation of cryptic unstable transcripts: a role for the nrd1-nab3 pathway in genome surveillance. *Mol Cell* **23:** 853–864

Vassylyev DG, Vassylyeva MN, Perederina A, Tahirov TH, Artsimovitch I (2007) Structural basis for transcription elongation by bacterial RNA polymerase. *Nature* **448:** 157–162

Westover KD, Bushnell DA, Kornberg RD (2004) Structural basis of transcription: nucleotide selection by rotation in the RNA polymerase II active center. *Cell* **119:** 481–489

Woychik NA, Lane WS, Young RA (1991) Yeast RNA polymerase II subunit RPB9 is essential for growth at temperature extremes. *J Biol Chem* **266:** 19053–19055

Woychik NA, Young RA (1989) RNA polymerase II subunit RPB4 is essential for high and low temperature yeast cell growth. *Mol Cell Biol* **9:** 2854–2859

Zaros C, Briand JF, Boulard Y, Labarre-Mariotte S, Garcia-Lopez C, Thuriaux P, Navarro F (2007) Functional organisation of the Rpb5 subunit shared by the three yeast RNA polymerases. *Nucleic Acids Res* **35:** 634–647

Zhang Z, Dietrich FS (2005) Mapping of transcription start sites in *Saccharomyces cerevisiae* using 5′ SAGE. *Nucleic Acids Res* **33:** 2838–2851